NÖHÜ Müh. Bilim. Derg. / NOHU J. Eng. Sci., 2023; 12(3), 912-918

Niğde Ömer Halisdemir Üniversitesi Mühendislik Bilimleri Dergisi
Niğde Ömer Halisdemir University Journal of Engineering Sciences

Araştırma makalesi / Research article

www.dergipark.org.tr/tr/pub/ngumuh / www.dergipark.org.tr/en/pub/ngumuh

Thermal buckling analysis of laminated plates with variable angle fiber orientation

Değişken fiber açılı kompozit plakların termal burkulma analizi

Fatih Baran[1], Demet Balkan[2,*]

[1,2] *Istanbul Technical University, Department of Aeronautics and Astronautics Engineering, 34469, İstanbul, Türkiye*

Abstract

The thermal buckling response of square plates with variable angle tows under simply supported conditions is modeled numerically. The path of variable angle tow is modeled as a function of lateral location. The classical lamination theory utilizes fiber paths to calculate thermal loads and stiffness matrices. Using Kirchhoff plate theory and finite element theory, the global material stiffness matrix and the global geometric stiffness matrix of the plate under thermal buckling loads are obtained. By using these matrices, eigenvalues or critical buckling temperature is obtained and the buckling response of the plate is examined. The theoretical results are validated by studies in the literature and finite element models. It has been seen even in an unoptimized span of a sample composite material, variable angle tows (VATs) were 8,60% more resistant to thermal buckling than common composite lay-ups.

Keywords: Variable angle tows, Thermal buckling, Composite plate buckling

Öz

Bu çalışmada, değişken açılı fiberlere sahip kare kompozit plakaların basit mesnet koşulu altında termal burkulma analizini yapmak için bir kod geliştirilmiştir. Değişken açılı fiberlerin oryantasyonu, yatay konumun bir fonksiyonu olarak modellenmiştir. Klasik laminasyon teorisi, termal yükleri ve direngenlik matrislerini hesaplamak için fiber yollarını kullanır. Khirchoff plaka teorisi ve sonlu elemanlar teorisinin modelleme yöntemleri kullanılarak, termal burkulma altındaki plakanın global malzeme rijitlik matrisi ve global geometrik rijitlik matrisi elde edilmiştir. Bu matrislere gerekli işlemler uygulanarak bu analiz için özdeğerler, yani kritik burkulma sıcaklığı elde edilebilir ve plakanın durumu yorumlanabilir. Sayısal çalışmadan elde edilen sonuçlar, literatürdeki çalışmalar ve sonlu eleman modelleri ile doğrulanmıştır. Örnek bir kompozit malzemenin optimize edilmemiş bir aralığında bile, değişken açılı kompozitlerin düz serimli kompozitlere göre termal burkulmaya karşı %8,60 daha dirençli olduğu görülmüştür.

Anahtar kelimeler: Değişken açılı kompozitler, Termal burkulma, Kompozit plaka burkulması

1 Introduction

Aircraft or spacecraft are exposed to temperature changes for various environmental reasons. As an example, the travel of high-speed aircraft in the atmosphere causes its temperature rises due to a phenomenon called aerodynamic heating [1]. Restrained from in-plane expansion, when geometrically perfect plates are heated slowly and uniformly, they usually develop compressive stresses and then buckle at a given temperature [2]. This temperature value is called the critical thermal buckling temperature and engineers have to consider this value in their designs, especially for aircraft operating at high Mach numbers. Some of the parts that are subject to thermal buckling are composite plates.

Composite materials have been used in many different areas from the past to the present. The main factors that make composite materials preferred and that are tried to be developed further and some properties which cause disadvantages are as in Table 1.

One of the disadvantages of composite material is that the direction is very important. While the mechanical values in the main direction are very good in classical fibers, the values in the lateral direction are relatively weak. Scientists and manufacturers have sought some ways to overcome this orientation problem and have found variable angle tow (VAT) as a solution.

Table 1. Material properties of composites [3]

Advantages	Disadvantages
Low specific weight *(ρ)*	Brittle
High specific stiffness *(E/ ρ)*	Limited shelf lives
High specific strength *(R/ ρ)*	Hard to storage
High resistance	Difficult to process material
Low thermal conductivity	Orientation is important

VATs are based on the principle that the fibers are placed in different orientations in the plane of each ply. The main purpose here is to achieve the optimum level by obtaining variable stiffness with variable angle tows. In this way, buckling resistance and resistance to other loads can also be improved [4].

* Sorumlu yazar / Corresponding author, e-posta / e-mail: kececidem@itu.edu.tr (D. Balkan)
Geliş / Recieved: 24.01.2023 Kabul / Accepted: 11.04.2023 Yayımlanma / Published: 15.07.2023
doi: 10.28948/ngmuh.1241416

The study of Gurdal et al. includes a path of fiber that has a function of both x and y. Classical lamination theory is used to get a stiffness matrix. In-plane and buckling analysis is done, and the Rayleigh-Ritz method is used for the eigenvalue. The pre-buckling analysis includes two cases; fiber orientation is a function of only x or only y. The simply supported plates are analyzed for these two cases, and the results are compared with the straight fibers [5].

Scientists from the University of Michigan; Duran et al. studied the thermal buckling response of a variable angle tow composite square plate. Since the geometry is square, their research is not dependent to aspect ratio. Similarly, to other studies, fiber angle is a function of position. The stacking sequence is restrained to be symmetric and balanced for this study. Simply supported square panels are used for analysis. Buckling analysis is done with out-of-plane equations. Results are found numerically, and the validation of this calculation is done with straight fibers. After that, the results are tried to be optimized with orientation changes. Finally, different material models are also examined [6].

In this study, it will be discussed what the response of different types of variable angle composites will be to the thermal buckling condition. The main scope will be developing a code which models the material and finds critical thermal buckling temperature at different conditions, validation will be done with the studies in the literature, and the finite element method models.

2 Modelling

2.1 Classical lamination theory

In order to model laminates, the relation of the lamina has to be defined. This process is explained by the classical lamination theory. Hooke's law for unidirectional lamina can be summarized as an equation below.

$$\begin{bmatrix}\sigma_1\\ \sigma_2\\ \tau_{12}\end{bmatrix}=\begin{bmatrix}Q_{11} & Q_{12} & 0\\ Q_{12} & Q_{22} & 0\\ 0 & 0 & Q_{66}\end{bmatrix}\begin{bmatrix}\varepsilon_1\\ \varepsilon_2\\ \gamma_{12}\end{bmatrix} \quad (1)$$

where,

$$Q_{11}=\frac{E_1}{1-\nu_{21}\nu_{12}} \qquad Q_{12}=\frac{\nu_{12}E_2}{1-\nu_{21}\nu_{12}} \quad (2)$$

$$Q_{22}=\frac{E_2}{1-\nu_{21}\nu_{12}} \qquad Q_{66}=G_{12} \quad (3)$$

By using equation above and orientation for laminas, separately, induced rigidity matrix $[\bar{\boldsymbol{Q}}]$ can be found.

$$[\bar{Q}]=\begin{bmatrix}\bar{Q}_{11} & \bar{Q}_{12} & \bar{Q}_{16}\\ \bar{Q}_{12} & \bar{Q}_{22} & \bar{Q}_{26}\\ \bar{Q}_{16} & \bar{Q}_{26} & \bar{Q}_{66}\end{bmatrix} \quad (4)$$

where,

$$\bar{Q}_{11}=Q_{11}c^4+Q_{22}s^4+2(Q_{12}+2Q_{66})s^2c^2 \quad (5)$$

$$\bar{Q}_{12}=(Q_{11}+Q_{22}-4Q_{66})s^2c^2+Q_{12}(s^4+c^4) \quad (6)$$

$$\bar{Q}_{22}=Q_{11}s^4+Q_{22}c^4+2(Q_{12}+2Q_{66})s^2c^2 \quad (7)$$

$$\bar{Q}_{16}=(Q_{11}-Q_{12}-2Q_{66})sc^3-(Q_{22}-Q_{12}-2Q_{66})s^3c \quad (8)$$

$$\bar{Q}_{26}=(Q_{11}-Q_{12}-2Q_{66})s^3c-(Q_{22}-Q_{12}-2Q_{66})sc^3 \quad (9)$$

$$\bar{Q}_{66}=(Q_{11}+Q_{22}-2Q_{12}-2Q_{66})s^2c^2+Q_{66}(s^4+c^4) \quad (10)$$

After the calculation of $[\bar{\boldsymbol{Q}}]$ for each ply, it is necessary to assemble the rigidity values of each lamina to get a unique stiffness matrix for laminate. This process is defined as the assembly of A-B-D matrices. These matrices are the functions of lamina thickness and height, and induced rigidity matrix $[\bar{\boldsymbol{Q}}]$ as seen in the equation for ***A-B-D*** matrices.

$$A_{ij}=\sum_{k=1}^{n}\left[(\bar{Q}_{ij})\right]_k(h_k-h_{k-1}) \quad (11)$$

$$B_{ij}=\frac{1}{2}\sum_{k=1}^{n}\left[(\bar{Q}_{ij})\right]_k(h_k^2-h_{k-1}^2) \quad (12)$$

$$D_{ij}=\frac{1}{3}\sum_{k=1}^{n}\left[(\bar{Q}_{ij})\right]_k(h_k^3-h_{k-1}^3) \quad (13)$$

After the calculation of ***A-B-D*** matrices, strains and curvatures under the applied force and moments can be found as equation below.

$$\begin{bmatrix}N\\ M\end{bmatrix}=\begin{bmatrix}A & B\\ B & D\end{bmatrix}\begin{bmatrix}\varepsilon\\ \kappa\end{bmatrix} \quad (14)$$

The strains and stresses are calculated for every h level of laminate, then the effects of hygrothermal states on force and moment components are emphasized. These effects can be classified into two groups. The first part, which is the main focus of this study, is the effects of temperature change. The second part is the moisture effect. These hygrothermal states mainly affect strains, and these will cause stress. All strain components can be stated in equation below.

$$\begin{bmatrix}\varepsilon_x\\ \varepsilon_y\\ \gamma_{xy}\end{bmatrix}=\begin{bmatrix}\varepsilon_x^M\\ \varepsilon_y^M\\ \gamma_{xy}^M\end{bmatrix}+\begin{bmatrix}\varepsilon_x^T\\ \varepsilon_y^T\\ \gamma_{xy}^T\end{bmatrix}+\begin{bmatrix}\varepsilon_x^C\\ \varepsilon_y^C\\ \gamma_{xy}^C\end{bmatrix} \quad (15)$$

M: Mechanical T: Thermal C: Moisture

Force effects of thermal situations are related to ***A*** matrice.

$$\begin{bmatrix}N_x^T\\ N_y^T\\ N_{xy}^T\end{bmatrix}=\Delta T\begin{bmatrix}A_{11} & A_{12} & A_{16}\\ A_{12} & Q_{22} & A_{26}\\ A_{16} & A_{26} & A_{66}\end{bmatrix}\begin{bmatrix}\alpha_1\\ \alpha_2\\ 0\end{bmatrix} \quad (16)$$

2.2 Variable angle path modelling

In this section, the fiber path difference of the composite layers is emphasized and as a result, appropriate modeling techniques are applied.

In section 2.1, it has been seen that stiffness values of ***A-B-D*** matrices have functions of material mechanical property, thickness, and laminate orientation stackings. There was no relation between lateral or longitudinal location and ***A-B-D*** matrices, since the fiber path is constant for in each lamina. In variable angle tows, the laminate will consist of a single lamina in the direction of thickness. However, the fiber path will have different orientation for lateral or longitudinal directions. In order to simplify modelling, the fiber path generally has a function of *x* direction (lateral). Fiber path is related to the *x* location by using edge and mid-orientations as in Figure 1 [6].

As a summary, the modelling can be formulated as in equation of $\theta(x)$, the illustration of equation can be examined in Figure 1.

$$\theta(x) = \begin{cases} \dfrac{2(\beta_1 - \beta_0)}{a}x + \beta_0, & 0 \le x < \dfrac{a}{2} \\ \dfrac{2(\beta_0 - \beta_1)}{a}x + \beta_0, & \dfrac{-a}{2} \le x < 0 \end{cases} \tag{17}$$

x: lateral direction

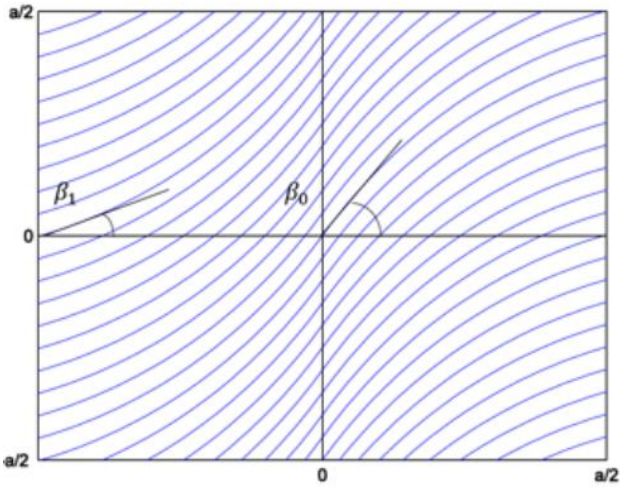

Figure 1. VAT orientation

2.3 Plate theory

The Classical Plate Theory (CPT) is obtained for isotropic materials by the Kirchhoff hypothesis. Kirchhoff's assumption is that if a plate deforms, midplane normals of the plate will remain straight and normal [7]. While the CPT is valid for thin panels, another plate theory, first order shear deformation theory (FSDT), also known as Mindlin plate theory, is suitable for thick plates. It calculates the rotations about *x* and *y* axis and the cross-sectional area does not have to remain normal for midplanes [8]. If x-y axis is located at midplane and *z* axes refers thickness axes, the kinematical behaviour of the plate is explained by Kirchhoff as in equation below.

$$u = u_0 - z\frac{\partial w}{\partial x} \qquad v = v_0 - z\frac{\partial w}{\partial y} \tag{18}$$

u, v, w: displacements of a typical point x,y,z respectively

u_0, v_0: displacements of a inplane point x,y respectively

The classical plane elasticity theory (CPET) states that there is a derivational relation between strain and displacement as seen in equation below.

$$\varepsilon_x = \frac{\partial u}{\partial x}\ , \qquad \varepsilon_y = \frac{\partial v}{\partial y}\ , \qquad \gamma_{xy} = \frac{\partial v}{\partial x} + \frac{\partial u}{\partial y} \tag{19}$$

The CPET can be applied if a composite structure has a single layer, or symmetrical multiple layers [7]. Under these conditions, buckling for simply supported composite plates can be governed by Von Karman's differential solutions as in equation below. If there is a coupling between bending and twist because of the unsymmetrical stacking, the additional $\boldsymbol{D_{16}, D_{26}}$ terms are also included in equation below.

$$\begin{aligned} D_{11}\frac{\partial^4 w}{\partial x^4} + 2(D_{12} + 2D_{66})\frac{\partial^4 w}{\partial x^2 \partial y^2} + D_{22}\frac{\partial^4 w}{\partial y^4} \\ = h\left(\sigma_x \frac{\partial^2 w}{\partial x^2} + 2\tau_{xy}\frac{\partial^2 w}{\partial x \partial y} \right. \\ \left. + \sigma_y \frac{\partial^2 w}{\partial y^2}\right) \end{aligned} \tag{20}$$

D_{ij}: Bending stiffness matrix $\quad h$: Thickness

3 Finite element theory

Buckling analysis includes several calculation steps. Since buckling is a stability problem, the geometry of structure has crucial importance. For instance, the analysis of columns and plates has huge differences since the stabilities of the structures are different because of the geometry. However, equation below can be used to generalize the buckling analysis [6].

$$\left|K_m + \lambda K_g\right| = 0 \tag{21}$$

K_m, K_g: Material and geometric stiffness matrices

λ: Buckling load factor

In the equation above, K_m is the material matrix that can be formulated as the equation below. K_m shows how resistant the structure is. K_m is widely used in static analysis and allows calculation of displacements and stresses on the body.

$$[K_m] = \int [B]^T [E][B] dV \tag{22}$$

B: Strain-displacement matrix, E: Material property matrix

$$[B]_{bend} = \begin{bmatrix} 0 & \dfrac{\partial N}{\partial x} & 0 \\ 0 & 0 & \dfrac{\partial N}{\partial y} \\ 0 & \dfrac{\partial N}{\partial y} & \dfrac{\partial N}{\partial x} \end{bmatrix} \tag{23}$$

and

$$[B]_{memb} = \begin{bmatrix} \frac{\partial N}{\partial x} & 0 \\ 0 & \frac{\partial N}{\partial y} \\ \frac{\partial N}{\partial y} & \frac{\partial N}{\partial x} \end{bmatrix} \quad (24)$$

Another stiffness matrix K_g is called the geometric stiffness matrix or the initial stress matrix. This matrix has no terms related to the mechanical properties of the material but depends on the geometric values and stresses on the body [9]. This matrix is a special matrix for buckling analysis, and its use is often different from K_m.

$$[K_g] = \int [G]^T [\sigma^0][G] dV \quad (25)$$

G: Geometry-displacement matrix, σ^0: Initial stress matrix

$$[G]_{bend} = \begin{bmatrix} \frac{\partial N}{\partial x} & 0 & 0 \\ \frac{\partial N}{\partial y} & 0 & 0 \end{bmatrix} \quad (26)$$

and

$$[G]_{shear} = \begin{bmatrix} 0 & \frac{\partial N}{\partial x} & \frac{\partial N}{\partial x} \\ 0 & \frac{\partial N}{\partial y} & \frac{\partial N}{\partial y} \end{bmatrix} \quad (27)$$

The calculation of the geometric stiffness matrix has same procedures with material stiffness matrix. Instead of strain-displacement matrix ***B*** and material matrix ***E***, geometric matrix ***G*** and initial stress matrix $\boldsymbol{\sigma^0}$ are used respectively. ***G*** matrix uses shape functions for contributions. $\boldsymbol{\sigma^0}$ matrix shows the effects of stress-state on the body. Generally, it is utilized to see permanent load effects [10].

Therefore, after determining the path of the fiber using edge and middle orientations for VAT modeling, ***A-B-D*** matrices and thermal loads are generated. To generate the material stiffness matrix and geometrical stiffness matrix, orientation and element stresses are utilized. Finally, the critical temperature of the system before buckling by calculating the buckling load factor can be estimated.

$$T_{critical} = \lambda T \quad (28)$$

4 Verification

Within the scope of this study, finite element based calculations made with the developed MATLAB code were verified using the results of finite element analysis and some studies in the literature. In the verification process, many cases are examined which isotropic materials under static loading, and thermal loading for cross-ply layup, angle-ply layup, and complex layup.

4.1 Isotropic plate

In this part, the results of the theoretical study, the analytical methods, and the FEM results are compared as an initial verification for buckling calculation. Shanmugam and Narayanan stated the buckling factor for the isotropic materials as in the reference [11].

$$\sigma_{cr} = k \frac{\pi^2 E}{12(1-\nu^2)} \left(\frac{t}{b}\right)^2 \quad (29)$$

An isotropic material with the below properties is used for verification. The analysis is carried out for a simply supported plate. In Table 2; a and b are plate length and width, k is the coefficient for simply supported plates, and σ is the compression stress which causes buckling.

Table 2. Material properties for isotropic verification

Property	Value
E (Elasticity M.)	70 GPa
ν	0.30
Length	1 m
Thickness	0.001 m
k	4.0 (SS)
$\sigma^0{}_{applied}$	1 MPa

The most critical eigenvalue for this geometry and material properties is shown in the table below. The error is based on the analytical formula σ_{cr} which is stated previously.

Table 3. Isotropic material verification

Analytical Formulation	The Code	FEM	Error of Code	Error of FEM
0.2530	0.2413	0.2587	4.62%	2.25%

Since the buckling calculation is verified under static loading, thermal loading can be examined. During the development of the finite element model in MSC Patran software, stress-induced distributed load and boundary conditions are applied as in Figure 2.

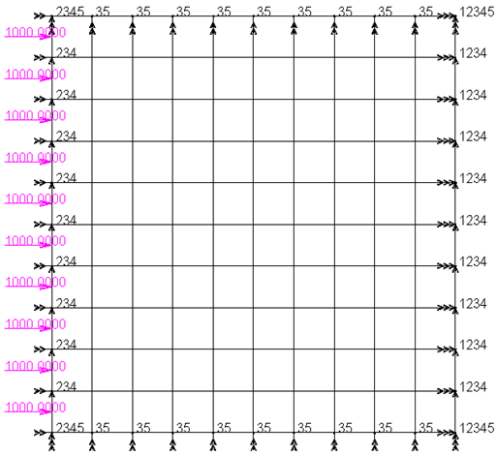

Figure 2. FEM for isotropic model

4.2 Composite plate

The theoretical results are obtained with the MATLAB code developed. Since the verification under thermal load is not easy with analytical formulas, literature studies and FEM results are used for verification. The theoretical study and FEM analysis are developed under a unit temperature change assumption as loading. Unit temperature loading was applied to uniform elements since it was desired to apply unit pressure, not a nodal force. The application on MSC Patran can be seen in Figure 3.

Figure 3. FEM for composite model

4.2.1 Cross ply-layup

As explained before, cross-ply refers to laminates which have *0°, 90°* orientation symmetrically. Different ply numbers are examined for a cross-ply layup. The theoretical results are compared with the study of Babu et al. [12].

Table 4. Properties of cross-ply layup

Property	Value
E (Elasticity M.)	$E_1/E_2 = 15$
Shear M.	$G_{12}/E_2 = 0.5$
ν_{12}	0.30
Thermal Exp. Coef.	$\alpha_1/\alpha_0 = 0.015$
Orientation	$[0/90]_s$
Length	0.15 m

The thermal forces acting on composite laminates are calculated by classical lamination theory for a given geometry and material properties. After that, the model with 6x6 elements is loaded by the calculated biaxial compression forces due to unit temperature change. The results for this case can be seen in Table 5. The study of Babu and Kant is based on error calculation.

Table 5. Cross-ply layup verification

a/h	Babu	The Code	FEM	Error of Code	Error of FEM
10	75.7	78.2	99.6	3.30%	31.5%
100	0.9960	0.9928	0.9959	0.32%	0.01%

*The correction parameter 10^3 is used for simplfication of results

As can be seen, the theoretical results obtained in this study are in good agreement with the results of the study of Babu et al. In order to see the continuance of eigenvalues, the critical 10 eigenvalues are elaborated. The results and errors for these cases can be seen in Table 6.

Table 6. Cross-ply layup 10 buckling mode

a/h	The Code	FEM	Error
1	0.9928	0.9959	0.32%
2	1.4499	1.4574	0.52%
3	2.8126	2.8123	0.01%
4	3.9976	4.0811	2.04%
5	4.5259	4.6546	2.76%
6	4.8030	4.4805	0.98%
7	4.9826	4.8951	1.78%
8	6.4601	6.5512	1.39%
9	8.1239	7.6320	6.44%
10	9.6869	9.5158	1.80%

4.2.2 Angle ply layup

In the present section, one of the very common orientation, *[45°,-45°. . .]* is focused. The same analysis is repeated with different layer numbers. The results for this case can be seen at Table 8. The study of Babu et al. is based on error calculation.

Table 7. Properties of angle-ply layup

Property	Value
E (Elasticity M.)	$E_1/E_2 = 15$
Shear M.	$G_{12}/E_2 = 0.5$
ν_{12}	0.30
Thermal Exp. Coef.	$\alpha_1/\alpha_0 = 0.015$
Orientation	$[45/-45/45/-45]$
Length	0.15 m

When we compare Table 5 and Table 8, it will be seen that angle-ply layups are more resistant to buckling for the same *a/h* ratio. The *a/h*=10 case has 3% error roughly, when the *a/h*=100 case has 12%.

Table 8. Angle-ply layup verification

a/h	Babu	The Code	FEM	Error of Code	Error of FEM
10	106.1	102.9	155.3	3.01%	46.3%
100	1.4680	1.6555	1.5560	12.8%	5.99%

*The correction parameter 10^3 is used for simplfication of results.

4.2.3 Complex ply layup

In this part, analysis is one step further complicated and a similar orientation with Duran's study is used [6]. Graphite-Epoxy is used to ensure compatibility with the other work. The material properties and geometry can be seen in Table 9.

By utilizing the information in the above table, the analysis process is done. The result of the code is compared with the study of Duran [6].

As can be seen from table Table 10, the error ratios are small and negligible. In this verification, both orientation and layer number complexity are tested for code.

To summarize, the error of the code for different types of composite layups and aspect ratios is tested. Error rates are acceptable, even below 1% in some cases. Therefore, the code can be used trustingly for common straight layups. Now, it is necessary to verify the variable angle capabilities of the code.

Table 9. Properties of complex-ply layup [6]

Property	Value
E_1	155 GPa
E_2	8.07 GPa
G_{12}	4.55 GPa
ν_{12}	0.22
α_1	$-0.07x10^{-6}$°C^{-1}
α_2	$30.1x10^{-6}$°C^{-1}
Orientation	$[45/-45/0/90]_s$
Length	0.15 m
Total thickness	1.016 mm

Table 10. Complex layup verification

Duran	The Code	FEM	Error of Code	Error of FEM
39.40	38.51	38.72	2.26%	1.72%

4.2.4 Variable angle tows

The used methods and result for the variable angled tows are verified by using the study of Duran. There are five different materials all have different edge and center orientations. In Table 11, mechanical properties of materials can be seen.

In Table 12, thermal properties and orientations of materials can be seen.

Table 11. Mechanical properties for VATs [6]

Material	E_1 [GPa]	E_2 [GPa]	G_{12} [GPa]	ν_{12}
E-Glass/ Epoxy	41	10.04	4.3	0.28
S-Glass/ Epoxy	45	11.0	4.5	0.29
Carbon/ Peek	138	8.7	5.0	0.28
Carbon/ Polyimide	216	5.0	4.5	0.25
Boron/ Epoxy	201	21.7	5.4	0.17

Table 12. Thermal properties for VATs

Material	α_1 [°C$^{-1}x10^{-6}$]	α_1 [°C$^{-1}x10^{-6}$]	Center Orientation	Edge Orientation
E-Glass/ Epoxy	7.0	26	6.71°	58.04°
S-Glass/ Epoxy	7.1	30	16.12°	54.74°
Carbon/ Peek	-0.2	24	63.07°	29.50°
Carbon/ Polyimide	0.0	25	56.30°	36.68°
Boron/ Epoxy	6.1	30	-6.57°	63.28°

All these cases are considered as a verification process of VAT. All cases cover the same geometrical properties are stated below. According to the result of this verification part, the usability of the code can be decided.

In the validation part of VATs, the error level is occurred around 2% except one case. This dispensation has 6% error which is under 10% and acceptable. Therefore, the code can be used for VATs with the support of these validations.

Table 13. VAT verification

Material	Duran	The Code	Error
E-Glass/ Epoxy	5.58	5.47	1.87%
S-Glass/ Epoxy	5.04	4.97	1.26%
Carbon/ Peek	38.08	35.56	6.60%
Carbon/ Polyimide	78.28	77.31	1.24%
Boron/ Epoxy	7.50	7.30	2.69%

5 Results

In this section, a sample composite material is selected and modeled as variable angle tow composite plates. Later, this model is compared with the straight-angle composite plates, with the same geometrical and material properties, and the effectiveness of the variable-angle composites is investigated.

One of the very common materials in the aviation industry, boron epoxy, is examined to show the effective buckling resistance of VATs. The necessary material properties for the analysis are taken from Table 11 and Table 12. The preferred geometry is generated with a ratio of *a/h*=100.

Each of the configurations is under a unit thermal load with the same geometrical and material properties. The only difference between the configurations is the orientation of laminates. Edge and center orientations are respectively for VATs.

Table 14. Buckling comparison of a VAT

	Common Layups		VAT	Increment
Orientation	$[0/90]_s$	$[45/-45]_s$	(5,-60)	
Eigen V.	10.2286	14.4204	15.6604	8.60%

In the comparison analysis, two common straight-angle layups which are $[0/90]_s$, $[45/-45]_s$are investigated. Under the given geometry, and material conditions with the given orientations, it is found that the VAT is 8.60% more effective than the $[45/-45]_s$layup (the most buckling resistant straight layup) and 53.10% more effective than $[0/90]_s$,layup. Even the VAT orientation is not optimized, in this case, buckling resistance is increased by approximately 10% compared to the most effective straight lay-up. This value can be increased by optimizing the VAT orientation.

6 Conclusion

In the presented study, a MATLAB code is developed to reveal whether the variable angle composite plates will be subjected to buckling under thermal load, and the load factor or critical temperature value is obtained. Simple support is preferred as the boundary condition of the plates, and analyses are carried out accordingly. Square-shaped plates are used as a geometric feature.

While modeling the plates, the classical lamination theory, which is the basis of composite materials, is used. With the help of this theory, the stiffness matrices (***A-B-D***) of the composites and the thermal loads they are exposed to under unit temperature are calculated. After the modeling of the plate, the solution block is set into the code as a matrix operation of material and geometrical stiffness values.

Many analyzes are carried out during the verification phase of the code developed in this study. The studies of Duran and Babu are used and comparisons are made with some analytical formulas. In the verification phase, the process is reached from simple to complex.

The cross-layup, angle-layup, and variable-angle (non-optimized) states of the plate are compared under the same geometric conditions using Boron/Epoxy material. Even in the unoptimized state, the variable angled configuration is found to be around 9% more effective against angled layup, which is the most resistant of the straight-angle layered states. This ratio can be improved by optimization analysis.

As a result of the study, it is seen that the buckling analysis depends on the a/h ratio, the orientation of the layers, and the elastic modulus of the material. It has been observed that variable-angled composites can easily outperform straight-angled composites in a thermal buckling factor. In future studies, different boundary conditions options, the possibility of compatibility with different geometric surfaces (rectangular plate), and analysis of plates with stiffener can be examined.

Conflict of interest

The authors declare that there is no conflict of interest.

Similarity rate (iThenticate): %14

References

[1] V. Halbmillion, High-speed aircraft and aerodynamic heating. The Scientific Monthly, 69, 173–179, 1949. https://www.jstor.org/stable/19673.

[2] R. M. Jones, Thermal buckling of uniformly heated unidirectional and symmetric cross-ply laminated fiber-reinforced composite uniaxial in-plane restrained simply supported rectangular plates. Composites Part A: Applied Science and Manufacturing, 36 (10), 2005. https://doi.org/10.1016/j.compositesa.2005.01.028.

[3] K. B. Armstrong, L. G. Bevan, W. F. Cole, In Care and repair of Advanced Composites, 2'nd Ed., SAE International, pp. 1–4, 2005.

[4] Z. Wu, P. M. Weaver, G. Raju, B. Chul Kim, Buckling analysis and optimisation of variable angle tow composite plates. Thin-Walled Structures, 60, 163–172, 2012. https://doi.org/10.1016/j.tws.2012.07.008.

[5] Z. Gurdal, B. F. Tatting, C. K. Wu, Variable stiffness composite panels: Effects of stiffness variation on the in-plane and buckling response. Composites Part A: Applied Science and Manufacturing, 39 (5), 911–922, 2008. https://doi.org/10.1016/j.compositesa.2007.11.015.

[6] A. V. Duran, N. A. Fasanella, V. Sundararaghavan, A. M. Waas, Thermal buckling of composite plates with spatial varying fiber orientations. Composite Structures, 124, 228–235, 2015. https://doi.org/10.1016/j.compstruct.2014.12.065.

[7] A. W. Leissa, Buckling of laminated composite plates and shell panels. Defence Technical Information Center, 1986.

[8] G. R. Liu, S. S. Quek, The finite element method: A practical course, Elsevier, 2014. https://doi.org/10.1016/C2012-0-00779-X.

[9] E. L. Wilson, Three-dimensional static and dynamic analysis of structures: A physical approach with emphasis on earthquake engineering. Computers and Structures, 1995.

[10] Scia Engineers, Initial stress. SCIA structural analysis software and design tools, https://help.scia.net/22.0/en/#analysis/nonlinear_analysis/beam_local_nonlinearity/initial_stress.htm, Accessed 07 June 2022.

[11] N. E. Shanmugam, R. Narayanan, Structural analysis. ICE Manual of Bridge Engineering, pp. 49-112, November 2008, https://www.icevirtuallibrary.com/doi/abs/10.1680/mobe.34525.0049.

[12] T. Kant, C. S. Babu, Thermal buckling analysis of skew fibre-reinforced composite and sandwich plates using shear deformable finite element models. Composite Structures, 49 (1), 77–85, 2000. https://doi.org/10.1016/s0263-8223(99)00127-0.